Ferroelectric charge order enhanced by magnetic frustration in dimer Mott insulators

Hiroki Gomi,[1,2] Takeshi J. Inagaki,[3] and Akira Takahashi[1,2]

[1]*Graduate School of Engineering, Nagoya Institute of Technology, Gokiso-Cho, Showa-ku, Nagoya 466-8555, Japan*

[2]*CREST, Japan Science and Technology Agency, Chiyoda-ku, Tokyo 102-0075, Japan*

[3]*Graduate School of Materials Science, Nara Institute of Science and Technology, Ikoma, Nara 630-0192, Japan*

(Received 20 July 2015; revised manuscript received 11 October 2015; published 6 January 2016)

We investigate the effect of magnetic frustration on the dielectric properties of dimer Mott insulators. We adopt the two-dimensional quarter-filled extended Hubbard model for κ-(BEDT-TTF)$_2X$ with an additional coupling with the dimer lattice motions, and numerically obtain the ground state. In the parameter range for strong magnetic frustration, an interdimer bond-length alternation mode that lifts the quasidegeneracy of classical spin configurations is strongly coupled to the electron system; this alternation mode occurs even with an extremely small electron-lattice coupling constant. Furthermore, the bond-length alternation induces in the dimers electric dipoles, which align along the same direction. A dimer Mott insulator phase with the ferroelectric charge order is obtained in the region. These results are consistent with the relaxorlike dielectric anomaly in κ-(BEDT $-$ TTF)$_2$Cu$_2$(CN)$_3$.

DOI: 10.1103/PhysRevB.93.035105

I. INTRODUCTION

The quantum spin liquid state is one of the fascinating themes in strongly correlated electron systems. Recently, a possibility for such states was proposed in κ-(BEDT $-$ TTF)$_2$Cu$_2$(CN)$_3$ because of the absence of a long-range magnetic order down to 32 mK [1–4]. Various unconventional properties stemming from large quantum spin fluctuations have attracted much attention.

(BEDT-TTF)$_2X$ (X is a monovalent anion) can be described as a quasi-two-dimensional strongly correlated electron system with a quarter-filled valence band in terms of holes. In κ-(BEDT-TTF)$_2X$, the BEDT-TTF molecular lattice is distorted to form dimers, and the hole orbitals of the two dimerized molecules are strongly hybridized. As a result, a dimer can be effectively treated as a single site, and κ-(BEDT-TTF)$_2X$ can be regarded as a half-filled system. κ-(BEDT-TTF)$_2X$ exhibits a Mott insulator phase if the Coulomb interaction energy $U^{(\mathrm{dim})}$ between the two holes in a dimer is larger than its critical value [5–8]. This kind of insulating state is called the dimer Mott insulator.

It is believed that the dimer sites form a nearly regular triangular lattice in κ-(BEDT $-$ TTF)$_2$Cu$_2$(CN)$_3$ [9], and the origin of the quantum-spin liquid nature has been ascribed to geometrical frustration from the triangular lattice. Many different theoretical works have been done on this problem using half-filled models on the triangular lattice. It has been shown successfully that a nonmagnetic, gapless phase is realized in a range of anisotropies in the spin-spin interaction constant [10–14].

Recently, a dielectric anomaly has been observed in κ-(BEDT $-$ TTF)$_2$Cu$_2$(CN)$_3$ [15], which shows that charge degrees of freedom are still active in contrast to the conventional Mott insulators. Besides the dielectric anomaly, some of the properties are considered to be related to the charge degrees of freedom: electronic optical components inside the Mott gap [16–21]; the broadening of some vibrational modes [22–24]; anomalies in the lattice expansion coefficient and specific heat at around 6 K [25–27]. The origins of these phenomena have been intensely discussed, and it has been proposed that they arise from electric dipoles in dimers [15–18,28,29]. Nevertheless, there are experimental results that show the absence of electric dipoles in dimers, where magnetic domain walls coupled with charges are attributed to the origin of the dielectric anomaly [30–34]. Controversy remains whether these electric dipoles in dimers actually exist.

Furthermore, the dielectric anomaly shows a possibility of electronic ferroelectricity [35–37] in κ-(BEDT $-$ TTF)$_2$Cu$_2$(CN)$_3$. In electronic ferroelectricity, where the electric polarization is governed by electrons, a large magnetodielectric coupling and a fast polarization switching are expected, and electronic ferroelectricity has attracted much attention because of these novel properties. Multiferroics [38–40] and charge-order-driven ferroelectricity [41–48] are representative examples of electronic ferroelectricity.

In the half-filled models, a dimer is considered as a unit, and the electric dipoles in dimers cannot be described. Regarding the electric dipoles in dimers, some theoretical studies have been done using the quarter-filled models, where a BEDT-TTF molecule is considered as a unit and intradimer degrees of freedom are taken into account. Effective Hamiltonians for the quarter-filled extended Hubbard model for κ-(BEDT-TTF)$_2X$ have been derived assuming very large $U^{(\mathrm{dim})}$, and it has been shown that the ferroelectric phase arising from electric dipoles in dimers does appear over some parameter range in these models [28,29]. Furthermore, the interactions between the electric dipoles in dimers and spins are included in these models, and the effect of dipolar spin coupling on the spin structure is discussed in these works. Also in the original extended Hubbard model, it has been shown that the ferroelectric dimer Mott insulator phase exists near the boundary with a metallic phase [16,49]. A similar ferroelectric dimer Mott insulator phase is found in the extended Hubbard model on a geometrically frustrated lattice, which is different from that of κ-(BEDT-TTF)$_2X$ [50].

The effects of strong geometrical frustration have been investigated extensively in the half-filled models on a triangular dimer lattice. However, the parameter regions where quantum spin fluctuations arising from geometrical frustration are strongly enhanced, have not been sufficiently analyzed

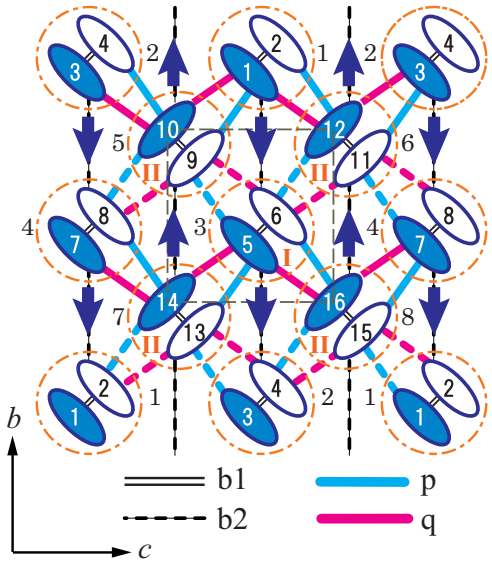

FIG. 1. The bond and charge structure when the lengths of p and q bonds alternate along the b axis. The ellipses and circles represent the BEDT-TTF molecules and the dimers, respectively, and the arrows show the direction of deviation of each dimer. The thick solid (thick dashed) lines show the p+ and q+ (p− and q−) bonds. The b1 and b2 bonds are marked by thin lines. The colored (white) ellipses represent the charge-rich (charge-poor) sites. A rectangle shows the unit cell, and the two dimers in the unit cell are labeled by I and II.

in the quarter-filled models, and the relationship between ferroelectricity and the large quantum spin fluctuations has yet to be clarified. We focus on this point in this paper. We find that even an extremely small perturbation of the electron-lattice coupling induces a ferroelectric dimer Mott insulator ground state in the parameter range where spin fluctuations are strongly enhanced as a result of strong geometrical frustration. Furthermore, we discuss the implications of the present results for the dielectric and magnetic properties of κ-(BEDT − TTF)$_2$Cu$_2$(CN)$_3$.

II. MODEL

We show the lattice structure of κ-(BEDT-TTF)$_2X$ in Fig. 1. We adopt the crystal axes for κ-(BEDT − TTF)$_2$Cu$_2$(CN)$_3$, and the b and c axes are defined as depicted in Fig. 1. As shown in the figure, there are four nonequivalent bonds, and they are labeled by b1, b2, p, and q according to Mori *et al.* [51]. The b1 bond is much stronger than the other ones, and the two BEDT-TTF molecules connected by the b1 bond form a dimer.

We consider only the lowest unoccupied molecular orbital of a BEDT-TTF molecule. Then, there is one orbital per lattice site, and the electron system is quarter-filled in regard to holes. We consider the quarter-filled extended Hubbard Hamiltonian for holes on a two-dimensional anisotropic triangular lattice.

We focus on the electron-lattice coupling with alternation modes of interdimer bond-lengths, which have predominant effects on the charge and spin structures of the ground state as will be shown later. There are two dimers in the unit cell, and they are labeled by I and II as shown in Fig. 1. By alternation of p and q bond lengths along the b axis (c axis), we mean the lattice deformation where dimers I and dimers II deviate by $\delta/2$ and $-\delta/2$, respectively, from their positions in a uniform dimer lattice, along the b axis (c axis), and $|\delta|$ gives the magnitude of the bond-length alternation. In Fig. 1, we mark with arrows the direction of deviation of the dimers when the lengths of p and q bonds alternate along the b axis.

Some p (q) bonds become shorter and the others become longer than those in the uniform lattice when bond-length alternation occurs. The shorter (longer) p and q bonds are denoted by p+ and q+ (p− and q−) bonds, respectively. When the lengths of p and q bonds alternate along the b axis, the p+ and q+ (p− and q−) bonds are shown by the thick solid (dashed) lines in Fig. 1. The b1 and b2 bond lengths are not altered by the bond-length alternation; these bonds are shown by the thin lines. The stretching modes of the b1 bonds play a crucial role in the photoinduced transition to a metallic phase [52–54], but their effects on the ferroelectric properties are much smaller than those considered here.

The extended Hubbard Hamiltonian coupled with the bond-length alternation mode is given by

$$H(\delta) = \sum_{\langle n,m\rangle,\sigma} t_{n,m}(c^{\dagger}_{m,\sigma}c_{n,\sigma} + c^{\dagger}_{n,\sigma}c_{m,\sigma}) + U\sum_{n} n_{n,\uparrow}n_{n,\downarrow} + \sum_{\langle n,m\rangle} V_{n,m}n_n n_m + NK\delta^2. \quad (1)$$

The first term describes the transfer of holes, where $\langle n,m\rangle$ denotes neighboring-site pairs, $c_{n,\sigma}$ ($c^{\dagger}_{n,\sigma}$) is the annihilation (creation) operator for a hole with spin σ at the site n, and $t_{n,m}$ is the transfer integral between the sites n and m. The electron-lattice coupling is included in this term as will be shown later. The second and third terms describe the on-site Coulomb interaction and the Coulomb interaction between the neighboring sites, respectively, where U is the on-site Coulomb interaction energy, $V_{n,m}$ is the Coulomb interaction energy between the sites n and m, $n_{n,\sigma} = c^{\dagger}_{n,\sigma}c_{n,\sigma}$, and $n_n = \sum_{\sigma} n_{n,\sigma}$. The fourth term shows the deformation energy of the p and q bonds, where we assume that the elastic coefficient K is the same for these bonds for simplicity. The number of p (q) bonds is equal to the system size N. The quantum effects of the lattice motion are not considered and the lattice degrees of freedom are described by the classical variable δ.

We take into account the δ dependence of $t_{n,m}$ only to first order assuming small $|\delta|$. Then, the transfer integrals $t_{\mathrm{p}\pm}$ and $t_{\mathrm{q}\pm}$ for the p± and q± bonds, respectively, are given by $t_{\mathrm{p}\pm} = t_{\mathrm{p}} \pm t'|\delta|$ and $t_{\mathrm{q}\pm} = t_{\mathrm{q}} \mp t'|\delta|$, where t_{p} (t_{q}) is the transfer integral for the p (q) bond in the uniform lattice, and t' is the absolute value of the differential coefficient of $t_{n,m}$. We here assume that the absolute values are the same for the p and q bonds for simplicity. As $t_{\mathrm{p}} > 0$ and $t_{\mathrm{q}} < 0$ hold, the signs of the first-order terms are given by the above equations. The transfer integral $t_{n,m}$ for the b1 (b2) bond for alternating bond-length is the same as that for the uniform lattice to first order in δ, and it is denoted by t_{b1} (t_{b2}). Because $V_{n,m}$ weakly depends on δ, we neglect the δ dependence of $V_{n,m}$. We denote $V_{n,m}$ by V_{p} if the sites n and m are connected by the p bond, and those for the other bonds are denoted similarly.

The electronic ground state $|\psi_0(\delta)\rangle$ of the Hamiltonian $H(\delta)$ is obtained by the rigorous diagonalization of $H(\delta)$. We further calculate the lattice distortion δ_0 that minimizes the energy of the electron-lattice coupled system from the self-consistency condition with lattice

$$\frac{\partial}{\partial\delta_0}\langle\psi_0(\delta_0)|H(\delta_0)|\psi_0(\delta_0)\rangle = 0. \tag{2}$$

Therefore $|\psi_0(\delta_0)\rangle$ is the ground state of the electron-lattice coupled system, and $|\psi_0(\delta_0)\rangle$ is simply denoted by $|\psi_0\rangle$ in the following.

To investigate the physical properties of $|\psi_0\rangle$, we numerically calculate a deviation of charge density from its mean value at the site n:

$$\rho_n = \langle\psi_0|n_n|\psi_0\rangle - 0.5, \tag{3}$$

the bond order

$$p_{n,m} = \sum_\sigma \langle\psi_0|c^\dagger_{n,\sigma}c_{m,\sigma}|\psi_0\rangle, \tag{4}$$

and the spin correlation

$$\eta_{n,m} = \langle\psi_0|\boldsymbol{S}_n\cdot\boldsymbol{S}_m|\psi_0\rangle, \tag{5}$$

between the sites n and m, where $\boldsymbol{S}_n$ is the spin operator at the site n. When the sites n and m are connected by, for example, a p+ bond, $p_{n,m}$ and $\eta_{n,m}$ are denoted by $p_{\mathrm{p}+}$ and $\eta_{\mathrm{p}+}$, respectively. Those for the other bonds are denoted in the same way.

Moreover, as there is one hole on each dimer, the spin structure is more clearly seen by considering a dimer as a unit. The dimer spin correlation $\eta_{l',l}$ between the dimer l and l' is defined by

$$\eta_{l',l} = \langle\psi_0|(\boldsymbol{S}_{2l'-1}+\boldsymbol{S}_{2l'})\cdot(\boldsymbol{S}_{2l-1}+\boldsymbol{S}_{2l})|\psi_0\rangle. \tag{6}$$

Note that two molecules at the sites $2l-1$ and $2l$ constitute the dimer l, as shown in Fig. 1. Here and hereafter, the molecular site numbers are denoted by n and m, and the dimer site numbers are denoted by l and l'. A diagonal (vertical) interdimer bond consists of p and q bonds (a b2 bond), and it is denoted by a D (V) bond. The dimer spin correlation η_{D} shows $\eta_{l',l}$ when the dimers l' and l are connected by a D bond, and those for the other bonds are denoted in the same way.

We consider the probability P_{s} that a dimer is singly occupied in $|\psi_0\rangle$. The ground state is given as a linear combination of basis states of the Hilbert space, and it can be written as

$$|\psi_0\rangle = \sum_{\{n_i,\sigma_i\}} C(\{n_i,\sigma_i\})\prod_{i=1}^{N/2} n_{n_i,\sigma_i}|\mathrm{vac}\rangle, \tag{7}$$

where $C(\{n_i,\sigma_i\})$ are the coefficients, $|\mathrm{vac}\rangle$ is the vacuum state. There are $N/2$ holes in the quarter-filled case. The probability P_{s} is given by the sum of $|C(\{n_i,\sigma_i\})|^2$ over the basis states where there is one hole at the dimer l (at the sites $2l-1$ and $2l$). Note that all the dimers are equivalent, and P_{s} does not depend on l. The relation $P_{\mathrm{s}}=1$ holds for the dimer Mott insulator in the strong correlation limit, and it is smaller than and close to 1 as a result of charge fluctuations with a realistic correlation strength.

For noninteracting cases $U = V_{\mathrm{b1}} = V_{\mathrm{b2}} = V_{\mathrm{p}} = V_{\mathrm{q}} = 0$, the ground states $|\varphi_i\rangle$ are 16-fold degenerate in energy with system size $N=16$, which is adopted for this study. As the Hückel band in the large N limit is partially filled, these 16-fold degenerate noninteracting ground states are metallic. We also consider the weight W_{m} of these 16 metallic states in $|\psi_0\rangle$, given by $W_{\mathrm{m}} = \sum_{i=1}^{16}|\langle\varphi_i|\psi_0\rangle|^2$.

III. RESULTS

We consider the 4×4 cluster of system size $N=16$, imposing periodic boundary conditions. To consider finite-size effects, we analyzed the results for dependence on three different periodic boundary conditions. For periodic boundary condition I (II), the 16-site clusters are tiled in a staggered manner along the c axis (b axis) to cover the anisotropic triangular lattice. In the condition III, the clusters are tiled without staggering. We show here the results with condition I because interdimer networks of important p and q bonds are in this case the longest. The shape of the cluster and the periodic boundary condition I are shown in Fig. 1. As will be shown later, the main conclusions are not altered by adopting different periodic boundary conditions, and this suggests that the finite-size effect is not serious in the present numerical calculations..

The transfer integrals for κ-(BEDT-TTF)$_2$Cu[N(CN)$_2$]Br have been calculated by the extended Hückel method [51]. We adopt them for t_{b1} and t_{b2}, and those scaled by a factor r for t_{p} and t_{q}: $t_{\mathrm{b1}}=0.265$, $t_{\mathrm{b2}}=0.074$, $t_{\mathrm{p}}=r\times0.109$, and $t_{\mathrm{q}}=r\times-0.038$. Hereafter, we use eV as the unit of energy. By changing the parameter r, the spin-spin interaction energy between the dimers connected by D bonds are changed, and the transitions between the Mott insulator states with different spin structures are induced, as will be shown later. We adopt the following Coulomb parameters appropriate for the κ-(BEDT-TTF)$_2X$: $U=0.7$, $V_{\mathrm{b1}}=0.45$, $V_{\mathrm{b2}}=V_{\mathrm{p}}=0.25$, and $V_{\mathrm{q}}=0.2$. Because the q bonds are significantly longer than the other interdimer bonds, we adopt the smaller value for V_{q}. The values for on-dimer Coulomb interaction energy $U^{(\mathrm{dim})}$, which is determined from U, V_{b1}, and t_{b1}, obtained in various references are largely different [7,8,55–57]. However, as long as the ground state is the dimer Mott insulator, the same results are obtained qualitatively using quite different values of $U^{(\mathrm{dim})}$. How these results depend on the interdimer Coulomb interaction parameters will be discussed later.

A. Ground-state properties in the absence of electron-lattice coupling

In this section, we show the results for $s=0$, where s is the electron-lattice coupling constant defined by $s=(t')^2/K$. In this case, $\delta_0=0$ holds and all the p and q bonds are equivalent for the ground state $|\psi_0\rangle$.

We show the r dependence of P_{s} and W_{m} for $0.3\leqslant r\leqslant1$ with the interval of 0.001 in Fig. 2. There are five phases, and at the four phase boundaries P_{s} and W_{m} change discontinuously with r. The phases for $r\geqslant0.998$, $0.997\geqslant r\geqslant0.463$, $0.462\geqslant r\geqslant0.453$, $0.452\geqslant r\geqslant0.451$, and $0.450\geqslant r$, are labeled I, II, III, IV, and V, respectively.

In phase I, W_{m} is about 0.5 and P_{s} is significantly smaller than those in the other phases. In phases II, III, IV, and V,

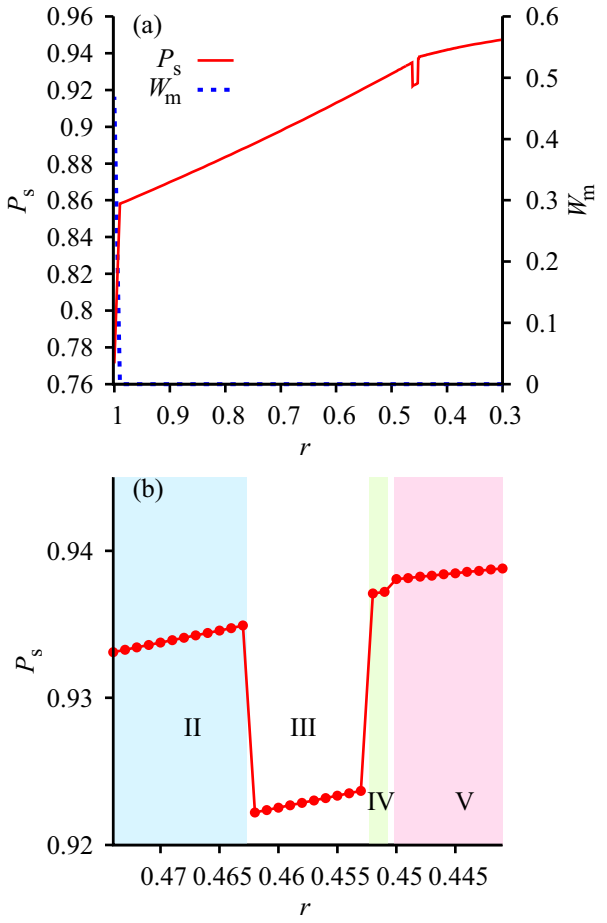

FIG. 2. The r dependence of P_s and W_m (a) for $0.3 \leqslant r \leqslant 1$ and (b) for $0.44 \leqslant r \leqslant 0.47$ ($W_m \approx 0$).

W_m is practically zero and P_s is very close to 1. Therefore we conclude that the ground state is metallic in phase I, and a dimer Mott insulator state in phases II, III, IV, and V.

The charge density is uniform in all the phases, but $\eta_{l',l}$ also changes discontinuously with r at the phase boundaries. We show $\eta_{l',l}$ for $r = 1$ (phase I), 0.463 (phase II), 0.452 (phase IV), and 0.450 (phase V) in Fig. 3. As all the dimers are equivalent, $\eta_{l',l}$ for all the dimer pairs are included in the figure. In phase II (V), $\eta_D < 0$ and $\eta_V > 0$ ($\eta_D = 0$ and

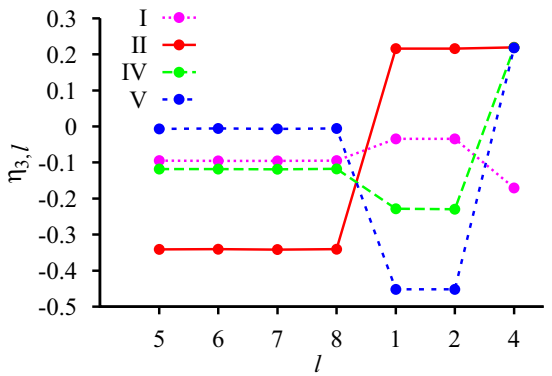

FIG. 3. The dimer spin correlation function $\eta_{3,l}$ for $r = 1$ (phase I), 0.463 (phase II), 0.452 (phase IV), and 0.450 (phase V).

$\eta_V < 0$) hold, where the dimers 3 and l are connected by a D (V) bond for $l = 5$, 6, 7, and 8 ($l = 1$ and 2) as seen in Fig. 1. The neighboring spin correlations for the ground state in phase II {V} are schematically shown in Fig. 4(a) [Fig. 4(b)]. In this figure, a dimer is considered as a unit with points and lines indicating dimers and interdimer bonds, respectively. The sign of $\eta_{l',l}$ between the dimers connected by a bond is shown by the line types of the bond. In addition to the strong dimer pair dependence of neighboring spin correlations, $\eta_{l',l} > 0$ holds and $|\eta_{l',l}|$ is not small for the second nearest-neighbor dimer pair 3 and 4 in phases II and V, (Fig. 3). Note that from Fig. 1, dimers 3 and 4 are the second-nearest neighbors. Therefore the ground states in phases II and V have antiferromagnetic (AFM) spin orders. Here, we do not mean that the long-range AFM spin order exists. Whether the long-range spin order exists or not cannot be inferred from the present results of small cluster calculations. The AFM spin order shows that holes are localized. Therefore this result is consistent with the conclusion that the ground state is a dimer Mott insulator state in phases II and V.

In each triangle of the dimer lattice, three neighboring spins cannot be pairwise anti-aligned. The signs of $\eta_{l',l}$ show that two spins connected by a D bond are antiparallel, and those by a V bond are parallel in the ground state of phase II. Two spins connected by a V bond and those by one of the two D bonds are antiparallel, and those by the other of the two D bonds are parallel in the ground state of phase V. There are degenerate classical spin states of this structure, and they are superposed in the ground state. Therefore η_V are zero in the ground state of phase V. The transfer integrals for κ-(BEDT-TTF)$_2X$ that exhibit AFM spin order have been calculated by an *ab initio* method [7,8] and the extended Hückel method [9,51]. The calculated anisotropy in the transfer integrals is consistent with the AFM spin order of phase II.

The magnitudes of spin correlations are much smaller in phases III and IV than in phases II and V. Because the probability P_s that a dimer is singly occupied is very close to 1, the Heisenberg spin Hamiltonian on the triangle dimer lattice is an appropriate effective Hamiltonian to describe the spin structures of the dimer Mott insulator ground states. We here consider the spin structures of these phases based on the effective model. The interaction between the two spins connected by a D bond is induced by the hole transfers of p and q bonds, and therefore the interaction energy J_D is proportional to r^2. That by a V bond is induced by the hole transfer of a b2 bond, and the interaction energy J_V is independent of r. The obtained spin structures show that $J_D > J_V$ ($J_D < J_V$) holds in the r region of phase II (V). Near the r region of phases III and IV, $J_D \simeq J_V$ holds, and geometrical frustration in the triangular dimer lattice is strongly enhanced. A large number of lowest energy classical spin states then have nearly the same energy expectation values, and these spin states are superposed with comparable weights in the ground state of phases III and IV as a result of the quasidegeneracy of the classical spin states. The small magnitudes for the spin correlations of the ground states in these phases are attributed to the large spin fluctuations arising from geometrical frustration.

We have confirmed this interpretation from the numerical results. In the ground states of phases III and IV, there are no dominant basis states, and a large number of basis states

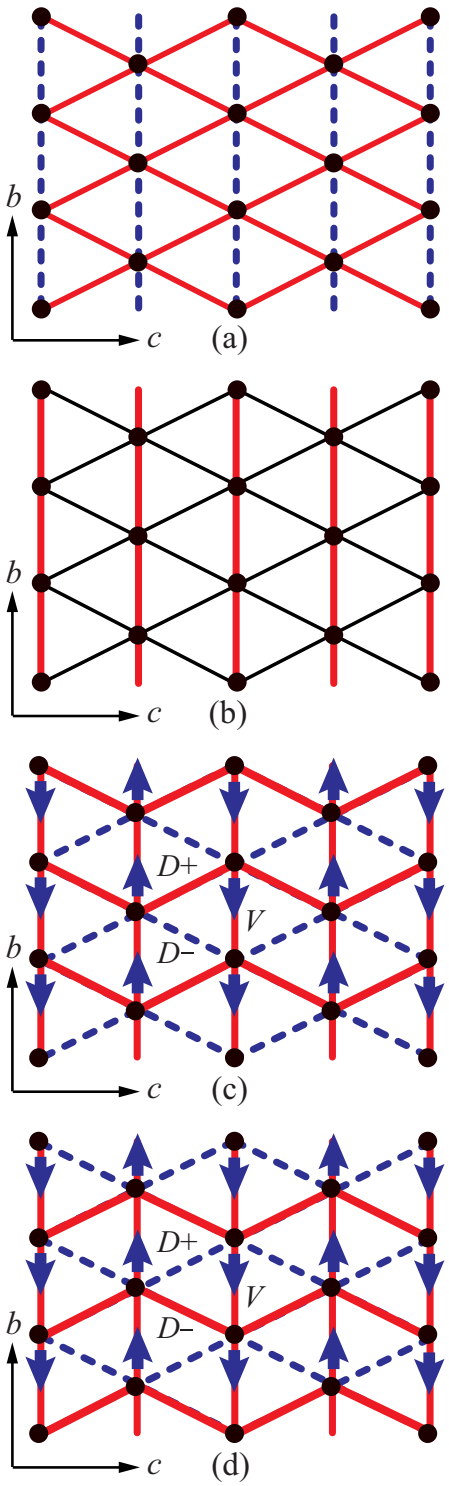

FIG. 4. The signs of the spin correlations between the neighboring dimers for the ground states in phases (a) II and (b) V in the absence of an electron-lattice interaction, and those for (c) the ferroelectric ground state and (d) the photoexcited state with $E_k - E_0 = 0.0104$ at $r = 0.458$ for an electron-lattice coupling of $s = 0.02$. The points show dimers, and the lines show the interdimer bonds. The relation $\eta_{l',l} < 0$ ($\eta_{l',l} > 0$) holds for dimers l' and l that are connected by a thick solid (dotted) line, and $\eta_{l',l} = 0$ holds for those connected by a thin solid line. The direction of deviation of the dimers when the lengths of p and q bonds alternate along the b axis, are shown by the arrows in (c) and (d).

with a variety of spin configurations on the dimer lattice have comparable $|C(\{n_i,\sigma_i\})|$.

The ranges of phases III and IV are extremely narrow, and this suggests that the energy differences between the dimer Mott insulator states of phases II, III, IV, and V are very small in the r region of these two phases. Therefore phases III and IV may not exist in the thermodynamic limit. However, we can safely say that the spin fluctuations are strongly enhanced near the r region between phases II and V, even in this case; this is a critically important point in understanding the ground-state properties in the electron-lattice coupling case. In our previous paper, we considered the parameter region around $r = 1$, with phase I (II) as the metallic (dimer Mott insulator) phase discussed in the paper [16,49].

B. Ground-state properties with electron-lattice interaction

In this section, we show the results for electron-lattice coupling $s > 0$. We numerically calculate the ground state in the parameter range $0.12 \geqslant s \geqslant 0$ and $0.8 \geqslant r \geqslant 0.3$. There is a critical value $s_c(r)$ for s. For $s < s_c(r)$, bond-length alternations do not occur, and the ground state $|\psi_0\rangle$ is the dimer Mott insulator with uniform charge, whereas for $s > s_c(r)$ the lengths for the p and q bonds alternate along the b axis. The lowest-energy state is always more stable when these lengths alternate along the b axis than when they alternate along the c axis over the same parameter range. Moreover, the charge structure of $|\psi_0\rangle$ always has the same pattern. The total charge of each dimer is zero, and an electric dipole moment is generated on each dimer. Also, the electric dipole moments on the dimers are aligned along the c axis (Fig. 1), and the electric polarization along this axis is induced by the bond-length alternation.

The magnitudes of the electric dipole moments are the same on all dimers and the charge density is the same at all the charge-rich (charge-poor) sites. Therefore the charge distribution of the ferroelectric ground state can be described by a single quantity ρ, which is the deviation of the charge density from its mean value at the charge-rich sites. We graphed ρ as a function of r and s (Fig. 5). In the area for which $\rho = 0$, bond-length alternation does not occur. In the

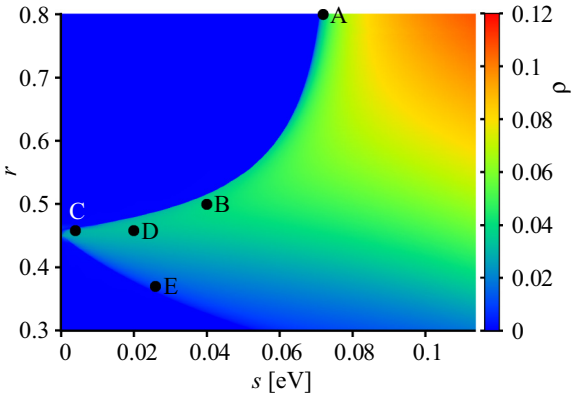

FIG. 5. Deviation of charge density from its mean value ρ (indicated by color scale) at the charge-rich sites as a function of r and s. Points A–E are explained in the text.

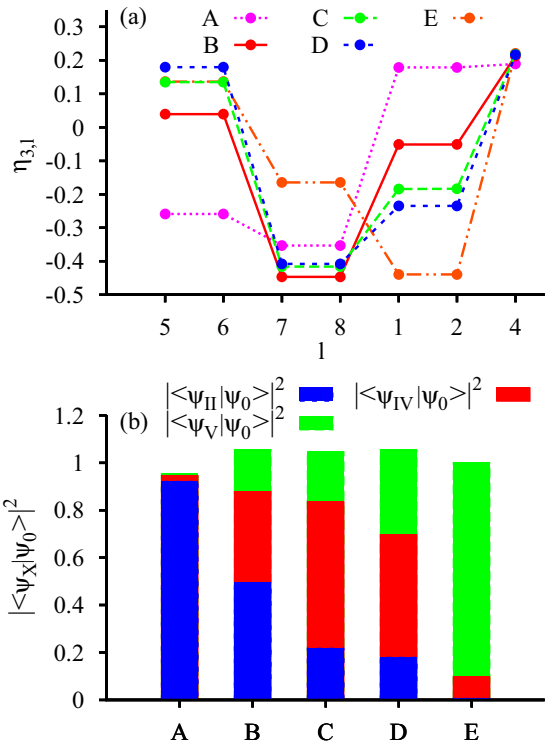

FIG. 6. (a) Dimer spin correlation function $\eta_{3,l}$ and (b) weight $|\langle\psi_{II}|\psi_0\rangle|^2$, $|\langle\psi_{IV}|\psi_0\rangle|^2$, and $|\langle\psi_V|\psi_0\rangle|^2$ at points A–E in the $r-s$ plane in Fig. 5

area of $\rho > 0$, the ground state is ferroelectric, and the lengths for the p and q bonds alternate along the b axis.

In a charge-ordered insulator α-(BEDT-TTF)$_2$I$_3$, the charge density depends sensitively on the electron-lattice coupling constant s, which for the b2 bond is estimated to be 0.06 eV from the charge distribution [58,59]. Unfortunately, it is difficult to estimate for κ-(BEDT-TTF)$_2X$ with its uniform charge density, but this value can be used as a rough estimation. As seen from this figure, $s_c(r)$ is much smaller than the estimated value near the r region of phases III and IV, where the spin fluctuations arising from geometrical frustration are strongly enhanced.

In Fig. 5, we consider the following points in the area of $\rho > 0$: A ($r = 0.8, s = 0.0720$), B ($r = 0.5, s = 0.0399$), C ($r = 0.458, s = 0.0024$), D ($r = 0.458, s = 0.0200$), and E ($r = 0.37, s = 0.026$). We plot the weights $|\langle\psi_{II}|\psi_0\rangle|^2$, $|\langle\psi_{IV}|\psi_0\rangle|^2$, and $|\langle\psi_V|\psi_0\rangle|^2$ at these points in Fig. 6(b), where $|\psi_{II}\rangle$, $|\psi_{IV}\rangle$, and $|\psi_V\rangle$ are the dimer Mott insulator ground states for $s = 0$ and $r = 0.463$ (phase II), 0.452 (phase IV), and 0.450 (phase V), respectively.

The matrix elements of $H(0)$ between the states $|\psi_{II}\rangle$, $|\psi_{IV}\rangle$, and $|\psi_V\rangle$ are almost equal to zero, but the lattice distortion allows these states to mix. As seen from Fig. 6(b), $|\langle\psi_{II}|\psi_0\rangle|^2 + |\langle\psi_{IV}|\psi_0\rangle|^2 + |\langle\psi_V|\psi_0\rangle|^2 \simeq 1$ holds for all the ferroelectric ground states $|\psi_0\rangle$, showing that $|\psi_0\rangle$ is approximately given by a linear combination of the dimer Mott insulator states $|\psi_{II}\rangle$, $|\psi_{IV}\rangle$, and $|\psi_V\rangle$ with different spin structures. As these states are not strictly orthogonal, the sum exceeds 1 in some ferroelectric states. This result clearly shows that the ferroelectric ground state $|\psi_0\rangle$ is a dimer Mott insulator. For the ferroelectric ground state, the weights change continuously with s and with r in contrast to the ground state associated with no electron-lattice interaction.

The weight $|\langle\psi_{III}|\psi_0\rangle|^2$ is zero over the r and s region considered. This is because the wave-number vector of $|\psi_{III}\rangle$ is different from those of the other dimer Mott insulator states. Recently, it has been shown that there exist various dimer Mott insulator phases with different spin structures between phases II and V from the mean-field calculations with large system size [60]. We believe phase III to correspond to one of these phases. The allowed wave-number vectors are restricted, and some of these phases cannot be described in the present small cluster calculations.

The spin structure of the ferroelectric ground state changes significantly as r changes. We show $\eta_{l',l}$ for $|\psi_0\rangle$ at points A, B, C, D, and E in Fig. 6(a). We first consider the r region of phases III and IV, where the ground state becomes ferroelectric even with an extremely small electron-lattice coupling constant s. Points C and D are in this region, and $s = 0.0024$ at the point C is much smaller than the other electric parameters. If lengths of p and q bonds alternate along the b axis, all the diagonal bonds are unequal, and each triangle of the dimer lattice consists of D+, D−, and V bonds, as shown in Fig. 4(c), where a diagonal interdimer bond that consists of the p+ and q+ (p− and q−) bonds is denoted by a D+ (D−) bond. The D+ (D−) bond is shorter (longer) than a D bond in the uniform lattice. In Fig. 6(a), $\eta_{3,l}$ is given as a function of l, and the dimers 3 and l are connected by a D+ bond for $l = 7$ and 8, by a D− bond for $l = 5$ and 6, and by a V bond for $l = 1$ and 2. At points C and D, $\eta_{D+} < 0$, $\eta_{D-} > 0$, and $\eta_V < 0$ hold. Furthermore, $\eta_{l',l} > 0$ holds and $|\eta_{l',l}|$ is not small for the second-nearest-neighbor dimer pairs. Therefore the ferroelectric ground state in this r region has AFM spin order; neighboring spin correlations are schematically shown in Fig. 4(c). The spin structure changes immensely by introducing an extremely small electron-lattice coupling. This can be confirmed from the weights shown in Fig. 6(b). Two dimer Mott insulator states $|\psi_{II}\rangle$ and $|\psi_V\rangle$ have significant weights in the ferroelectric ground states at points C and D in the r region of phases III and IV.

This predominant electron-lattice coupling can be understood based on the Heisenberg spin Hamiltonian on the triangle dimer lattice. As mentioned before, in the absence of electron-lattice interaction, a large number of classical spin states are quasidegenerate in energy in the r region of phases III and IV, where $J_D \simeq J_V$ holds, and they are superposed with comparable weights in the ground state. If the lengths of p and q bonds alternate along the b axis, $|t_{p+}| > |t_{p-}|$ and $|t_{q+}| > |t_{q-}|$ hold. Then, $J_{D+} > J_V > J_{D-}$ holds, where J_{D+} (J_{D-}) is the spin-spin interaction constant for a D+ (D−) bond, and the quasidegeneracy is lifted by the difference between the spin-spin interaction constants. As a result, the weights of these classical spin states are significantly changed, and the AFM ground state with neighboring spin correlations shown in Fig. 4(c) is attained. In this way, the bond-length alternation mode is strongly coupled with the electronic degrees of freedom, and this alternation occurs even with extremely small s under strong geometrical frustration.

In contrast, if the lengths of p and q bonds alternate along the c axis, each triangle consist of two D+ bonds and one V bond, or two D− bonds and one V bond, and therefore, a lift

of the quasidegeneracy does not occur. As a result, for the bond-length alternation mode the coupling is not very strong.

The magnitude of the bond order indicates the bond strength. The difference between t_{p+} and t_{p-} (t_{q+} and t_{q-}) also results in a difference in bond order, and $|p_{p+}| > |p_{p-}|$ ($|p_{q+}| > |p_{q-}|$) holds. As a result (Fig. 1), a site (the other site) in a dimer shown by the colored (white) ellipse is connected by three (one) stronger bonds and one (three) weaker bond. Because holes are more stabilized on stronger bonds, the sites shown by the colored (white) ellipses become charge-rich (charge-poor), and the electric dipoles in dimers are generated. Furthermore, the electric dipole moments are aligned along the c axis. With the same stabilization mechanism, a dimer Mott insulator phase with disproportionate charges in the dimers has been found also in the one-dimensional case [46,61,62].

Consequently, alternation of p and q bond lengths along the b axis induces both the AFM spin order with neighboring spin correlations, schematically shown in Fig. 4(c), and the differences between p_{p+} and p_{p-} and between p_{q+} and p_{q-}, which result in ferroelectric charge order. In this way, the spin and charge structures are coupled, and the ground state becomes the dimer Mott insulator with a ferroelectric charge order even by introducing an extremely small electron-lattice coupling constant s.

We next consider the r region of phase II (V). As r increases (decreases) from the value at the boundary with phase III (IV), $|\langle\psi_{II}|\psi_0\rangle|^2$ ($|\langle\psi_V|\psi_0\rangle|^2$) increases, the difference between η_{D+} and η_{D-} becomes smaller, and η_V increases (decreases). From Fig. 6(b), the weight of $|\psi_{II}\rangle$ ($|\psi_V\rangle$) is dominant in the ferroelectric ground state, which has the characteristic spin structure of phase II (V) at point A (E), which is far from the boundary with phase III (IV).

The energy gain per site Δe as a consequence of symmetry breaking of the bond-length alternation is given by

$$\Delta e = \frac{1}{N}(\langle\psi_0(0)|H(0)|\psi_0(0)\rangle - \langle\psi_0(\delta_0)|H(\delta_0)|\psi_0(\delta_0)\rangle). \quad (8)$$

Furthermore, to understand the stabilization mechanism, we consider the energy gains of various parts of the Hamiltonian: the transfer term H_t, the electron-lattice coupling term H_{e-l}, the on-dimer Coulomb interaction term H_{od}, and the interdimer Coulomb interaction term H_{id}, given by

$$H_{e-l}(\delta) = \sum_{\langle n,m\rangle,\sigma}^{\langle n,m\rangle\in p+,q-} t'|\delta|(c^\dagger_{m,\sigma}c_{n,\sigma} + c^\dagger_{n,\sigma}c_{m,\sigma}) - \sum_{\langle n,m\rangle,\sigma}^{\langle n,m\rangle\in p-,q+} t'|\delta|(c^\dagger_{m,\sigma}c_{n,\sigma} + c^\dagger_{n,\sigma}c_{m,\sigma}), \quad (9)$$

$$H_t = \sum_{\langle n,m\rangle,\sigma} t_{n,m}(c^\dagger_{m,\sigma}c_{n,\sigma} + c^\dagger_{n,\sigma}c_{m,\sigma}) - H_{e-l}(\delta), \quad (10)$$

$$H_{od} = U\sum_n n_{n,\uparrow}n_{n,\downarrow} + \sum_{\langle n,m\rangle}^{\langle n,m\rangle\in b1} V_{n,m}n_n n_m, \quad (11)$$

$$H_{id} = \sum_{\langle n,m\rangle} V_{n,m}n_n n_m - \sum_{\langle n,m\rangle}^{\langle n,m\rangle\in b1} V_{n,m}n_n n_m, \quad (12)$$

where $\sum_{\langle n,m\rangle}^{\langle n,m\rangle\in p+,q-}$ ($\sum_{\langle n,m\rangle}^{\langle n,m\rangle\in b1}$) denotes the summation over neighboring site pairs connected by the p+ and q− (b1) bonds.

The energy gain per site of H_{e-l} is given by

$$\Delta e_{e-l} = \frac{1}{N}(\langle\psi_0(0)|H_{e-l}(0)|\psi_0(0)\rangle - \langle\psi_0(\delta_0)|H_{e-l}(\delta_0)|\psi_0(\delta_0)\rangle), \quad (13)$$

and the energy gains of the other terms are denoted in the same way. The relation $\Delta e_{id} > 0$ holds, and the interdimer Coulomb interaction term contributes significantly to stabilize the ferroelectric phase. However, the formation of ferroelectric charge order always results in an increase in the on-dimer Coulomb interaction energy, and the relation $\Delta e_t + \Delta e_{od} + \Delta e_{id} < 0$ holds within a realistic parameter region. This is the reason why the dimer Mott ground state with ferroelectric charge order is not obtained without electron-lattice coupling in this parameter region.

Furthermore, we have analyzed the results for $V_p = V_q = V_{b2} = 0$ in the same way. Also in this case, the dimer Mott insulator ground state becomes ferroelectric even with extremely small values of s near the r region between phases II and V. Specifically, the ferroelectric dimer Mott insulator phase is obtained without the interdimer Coulomb interaction. Consequently, the strong electron-lattice coupling induced by geometrical frustration is relevant to stabilize the ferroelectric dimer Mott insulator phase obtained in this analysis. This is in contrast to the previously obtained phase stabilized mainly by the interdimer Coulomb interaction [28,29].

The energy gain Δe increases as the electron-lattice coupling constant s increases. For $r = 0.458$, where geometrical frustration is strong, $\Delta e = 1.5$, 3.7, and 6.5 K at $s = 0.02$, 0.04, and 0.06 eV, respectively. The energy gain Δe is very small even in reasonable regions of s. This comes from the characteristic electron-lattice coupling for strong geometrical frustration. The electron-lattice coupling mainly arises from lifting of the quasidegeneracy of a large number of classical spin states. Therefore even when the electronic structure is significantly changed by bond-length alternation, Δe is still small. This is closely related to the dielectric and magnetic properties of κ-$(BEDT-TTF)_2Cu_2(CN)_3$ to be discussed below.

Here, we comment on how the results depend on the periodic boundary conditions. The ferroelectric dimer Mott insulator phase is attained with even extremely small s in the r region between phases II and V also with periodic boundary conditions II and III. Furthermore, the spin correlation functions of the ferroelectric dimer Mott insulator ground states are almost the same between the three different periodic boundary conditions. These results suggest that ferroelectric dimer Mott insulator phase and the stabilization mechanism of the phase are robust against finite-size effects.

C. In-gap photoexcited states

We next consider the optical conductivity $\sigma_b(\omega)$ ($\sigma_c(\omega)$) from the ferroelectric ground state in the r region of phases III and IV when light is polarized along the b (c) axis. We show $\sigma_b(\omega)$ and $\sigma_c(\omega)$ at point D in Fig. 7(a). Here, δ is fixed to δ_0, and the contribution of lattice excitation is not considered. There is a Mott gap in $\sigma_b(\omega)$ and $\sigma_c(\omega)$, and we show the in-gap region. As seen from this figure, there are small peaks in the region. The spectral widths for the in-gap peaks arise from the

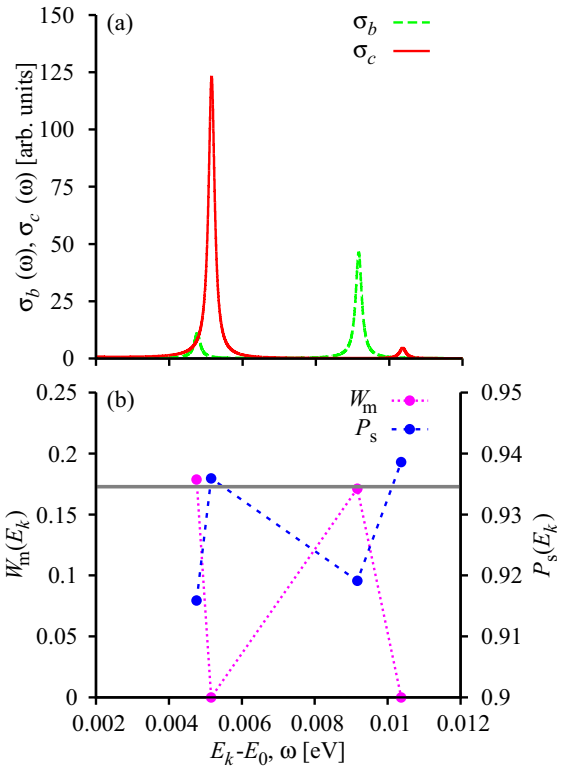

FIG. 7. (a) Optical conductivities $\sigma_b(\omega)$ and $\sigma_c(\omega)$ when light is polarized along b and c axis, respectively, and (b) $P_s(E_k)$ and $W_m(E_k)$ at point D. The horizontal line in (b) shows P_s for the ground state.

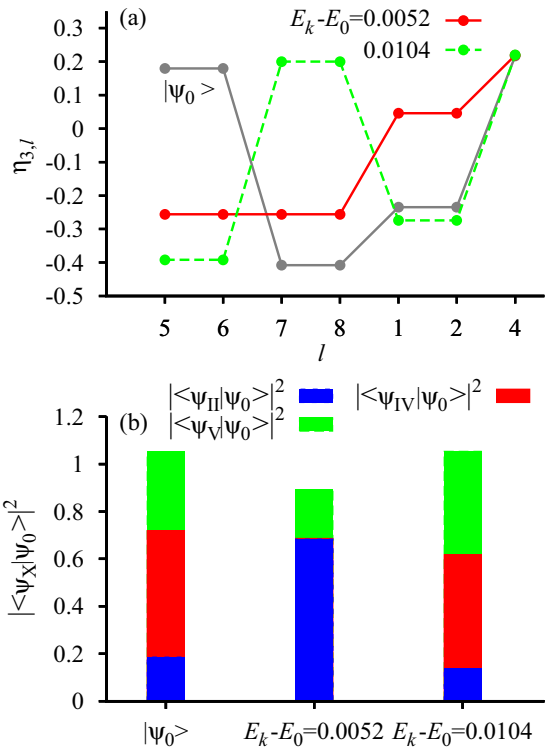

FIG. 8. (a) Dimer spin correlation functions $\eta_{3,l}$, and (b) $|\langle\psi_{II}|\psi_0\rangle|^2$, $|\langle\psi_{IV}|\psi_0\rangle|^2$, and $|\langle\psi_V|\psi_0\rangle|^2$ for $|\psi_k\rangle$ with $E_k - E_0 = 0.0052$, for $|\psi_k\rangle$ with $E_k - E_0 = 0.0104$, and for $|\psi_0\rangle$ at point D.

artificial broadening factor ϵ, which is used for convergence of the numerical calculations, and each peak at $\omega = E_k - E_0$ arises from the excitation to a single energy eigenstate $|\psi_k\rangle$ of $H(\delta_0)$ for the energy eigenvalue E_k, where E_0 is the energy eigenvalue of the ground state.

We numerically calculate in-gap energy eigenstates $|\psi_k\rangle$ using the method detailed in our previous paper [63], and show the probability $P_s(E_k)$ that a dimer is singly occupied, and the weight $W_m(E_k)$ of the 16 degenerate metallic ground states in the noninteracting case for $|\psi_k\rangle$ in Fig. 7(b). The probability $P_s(E_k)$ is larger than that of the ground state, and $W_m(E_k)$ is practically zero for the peaks in $\sigma_c(\omega)$. These results show that the peaks arise from the excitation to dimer Mott insulator states. In contrast, $P_s(E_k)$ is significantly smaller than that of the ground state, and $W_m(E_k)$ is comparable to that for the metallic ground state of phase I for the peaks in $\sigma_b(\omega)$. These results show that the peaks arise from the excitation to metallic states.

We focus on the peaks in $\sigma_c(\omega)$. We show $\eta_{l',l}$ for $|\psi_k\rangle$ that is responsible for these peaks, and the weights $|\langle\psi_{II}|\psi_k\rangle|^2$, $|\langle\psi_{IV}|\psi_k\rangle|^2$, and $|\langle\psi_V|\psi_k\rangle|^2$ in Fig. 8. The weight of $|\psi_{II}\rangle$ is dominant in $|\psi_k\rangle$ with $E_k - E_0 = 0.0052$; the state has the characteristic AFM spin structure of phase II. The weights for $|\psi_k\rangle$ with $E_k - E_0 = 0.0104$ are similar to those for the ground state, but $\eta_{l',l}$ for the state is essentially different from that for the ground state. The neighboring spin correlations of the state are schematically shown in Fig. 4(d). The sign of η_{D+} and that for η_{D-} are reversed from those for the ground state. Reflecting the spin structure, the sites shown by the white (colored) ellipses in Fig. 1 become charge-rich (charge-poor). The photoexcited state is polarized along the c axis, and the magnitude of the polarization is almost the same as that of the ground state but the direction is opposite to that of the ground state.

The in-gap peaks arise from excitations to dimer Mott insulator states with different spin structures, and these excitations become photoactive as a result of the coupling between the electric dipole moments on the dimers and spin degrees of freedom. They correspond to pure spin excitations, and the in-gap charge excitations do not exist in conventional Mott insulators without the coupling.

Furthermore, note that $|\langle\psi_{IV}|\psi_0\rangle|^2$ and $|\langle\psi_{IV}|\psi_k\rangle|^2$ with $E_k - E_0 = 0.0104$ are both nearly equal to 0.5. This shows that the dimer Mott insulator states with the two largely different neighboring spin correlations, schematically shown in Figs. 4(c) and 4(d), are superposed and have dominant weights in the ground state of phase IV for $s = 0$. This result supports the conclusion drawn about the origin of the strong electron-lattice coupling with the alternation mode of p and q bonds along the b axis. The bond-length alternation lifts the quasidegeneracy of a large number of classical spin states for the uniform lattice, as previously mentioned. The ground state $|\psi_0\rangle$ ($|\psi_k\rangle$ with $E_k - E_0 = 0.0104$) mainly consists of quasidegenerate spin states, the energies of which become lower (higher) as a result of bond-length alternation. Indeed, $E_k - E_0$ is roughly proportional to δ_0.

IV. DISCUSSION

We discuss the implications of the present results for the dielectric and magnetic properties of κ-(BEDT − TTF)$_2$Cu$_2$(CN)$_3$. The Curie-Weiss behavior is observed in the temperature T dependence of the low-frequency dielectric constant, and the Curie temperature T_c is estimated to be 8–9 K in κ-(BEDT − TTF)$_2$Cu$_2$(CN)$_3$ [15]. This result shows that the ferroelectric charge fluctuation is significant in this material but the existence of bulk ferroelectric charge order is not. In contrast, the ground state obtained in the present small cluster calculations has a ferroelectric charge order and AFM spin order. However, this inconsistency is resolved by considering the thermodynamic limit as will be shown below.

The ferroelectric ground state obtained in the present small cluster calculations is two-fold degenerate. The two degenerate states have opposite polarization directions and opposite phases of the bond-length alternation (opposite signs of δ). In the r region of strong geometrical frustration, because the energy gain per site Δe from symmetry breaking of the bond-length alternation is very small, the domain wall energy between these two degenerate ferroelectric phases will be very small. As a result, the domains of these two phases are generated by quantum fluctuations, and the ferroelectric charge order will be destroyed in the thermodynamic limit. As the domain fluctuation cannot be described in the small cluster calculations, a dimer Mott insulator ground state with ferroelectric charge order is obtained in the present calculations. Near $r = 0.5$ (B point), η_V is nearly equal to zero, showing that spin order along the vertical direction does not exist. Furthermore, as the D+ bonds with antiparallel spin correlations and the D− bonds with parallel spin correlations are reversed for the two degenerate ferroelectric states, the long-range spin order along the diagonal direction will be destroyed under quantum domain fluctuations. Consequently, in the thermodynamic limit, neither the long-range ferroelectric charge order nor the AFM spin order will exist but the ferroelectric charge fluctuation is significant in the ground state of the present model near $r = 0.5$. These properties are consistent with the dielectric property and the spin liquid nature of the material.

Next, we consider the finite-temperature properties of the model from the present zero-temperature results. The ferroelectric phase obtained in the present zero-temperature calculation is stable against thermal excitation if T is significantly smaller than Δe. Therefore thermal ferroelectric charge fluctuations are strongly enhanced for $T \simeq \Delta e$, and the Curie temperature T_c in the present model can be roughly estimated by Δe. As mentioned before, Δe for reasonable s in the r region of strong magnetic frustration is very small and roughly agrees with the experimentally estimated T_c. Therefore the small Δe obtained in the present model is consistent with the experimental data.

The bond-length alternation, which will affect the lattice expansion, occurs for $T < T_c$ in our scenario, and T_c is close to 6 K, for which anomalies in the lattice expansion coefficient and specific heat are observed [25–27]. We therefore consider that the anomalies can be explained from the transition between the bond-length alternated dimer Mott insulator state and that with uniform lattice. However, there have been no experimental results showing that bond-length alternation occurs. As mentioned before, the domains with opposite directions of lattice distortion are generated by quantum domain fluctuations. This discrepancy can be attributed partly to small domain size. Furthermore, the lattice distortion $\delta/2$ is less than 0.01 Å for $s \leqslant 0.05$, where we set K to 1.66 eV Å^{-2} used in Ref. [54], and the distortion may be too small to observe it experimentally.

A dielectric anomaly is observed also in the dimer Mott insulator β'-(BEDT-TTF)$_2$ICl$_2$ with square-lattice AFM spin order [64]. We consider that these experimental results can be explained from the ground-state properties of the present model for weak geometrical frustration. Even in the r region far from the phase boundaries, the critical electron-lattice coupling $s_c(r)$ is still in reasonable range, as seen in Fig. 5. Furthermore, in the ground state for $s > s_c(r)$ in the r region of phase II far from the phase boundary, η_{D+} and η_{D-} are different, which results in an electric polarization, but the signs are the same as seen from $\eta_{l',l}$ at point A shown in Fig. 6. This is because the effects of geometrical frustration are much smaller and the spin structure is not significantly changed by bond-length alternation in the region. That is, the two degenerate ferroelectric ground states have similar spin correlations. Therefore the domain fluctuation will destroy the ferroelectric charge order but will not destroy the spin order in the thermodynamic limit. The dielectric anomaly from the ferroelectric charge fluctuation and the AFM spin order are compatible for weak geometrical frustration. We believe the dielectric anomaly of β'-(BEDT-TTF)$_2$ICl$_2$ corresponds to this case.

There is a broad in-gap peak in $\sigma_c(\omega)$ that grows markedly at low temperature and saturates near T_c in κ-(BEDT − TTF)$_2$Cu$_2$(CN)$_3$ [17]. This shows that the peak is closely related to the ferroelectric charge fluctuation in the ground state. We believe the peak is assigned to the peak at $\omega = 0.0104$ in $\sigma_c(\omega)$ shown in Fig. 7(a). As shown in the previous section, $|\psi_0\rangle$ and $|\psi_k\rangle$ with $E_k - E_0 = 0.0104$ are superposed in the ground state of a uniform lattice, and they split as a result of bond-length alternation. Therefore the peak does not exist in the dimer Mott insulator ground states of the uniform lattice. As T increases to T_c, the ferroelectric domains generated by thermal fluctuations grow in the dimer Mott insulator phase with uniform charge, and therefore this peak grows. The characteristic T dependence can be explained from this.

V. CONCLUSION

In the parameter range of strong magnetic frustration, because the alternation of p and q bond-lengths along the b axis lifts the quasidegeneracy of the classical spin configurations, the bond-length alternation mode is strongly coupled to the electron system, and this alternation occurs even with an extremely small electron-lattice coupling constant. Furthermore, the bond-length alternation induces electric dipole moments on the dimers, which align along the c axis, and the dimer Mott insulator phase with ferroelectric charge order is attained in the region. These results are consistent with the relaxorlike dielectric anomaly in κ-(BEDT − TTF)$_2$Cu$_2$(CN)$_3$.

[1] Y. Shimizu, K. Miyagawa, K. Kanoda, M. Maesato, and G. Saito, Phys. Rev. Lett. **91**, 107001 (2003).

[2] S. Yamashita, Y. Nakazawa, M. Oguni, Y. Oshima, H. Nojiri, Y. Shimizu, K. Miyagawa, and K. Kanoda, Nat. Phys. **4**, 459 (2008).

[3] M. Yamashita, N. Nakata, Y. Kasahara, T. Sasaki, N. Yoneyama, N. Kobayashi, S. Fujimoto, T. Shibauchi, and Y. Matsuda, Nat. Phys. **5**, 44 (2009).

[4] A. P. Ramirez, Nat. Phys. **4**, 442 (2008).

[5] H. Kino and H. Fukuyama, J. Phys. Soc. Jpn. **64**, 2726 (1996).

[6] H. Kino and H. Fukuyama, J. Phys. Soc. Jpn. **65**, 2158 (1996).

[7] H. C. Kandpal, I. Opahle, Y.-Z. Zhang, H. O. Jeschke, and R. Valentí, Phys. Rev. Lett. **103**, 067004 (2009).

[8] K. Nakamura, Y. Yoshimoto, T. Kosugi, R. Arita, and M. Imada, J. Phys. Soc. Jpn. **78**, 083710 (2009).

[9] T. Komatsu, N. Matsukawa, T. Inoue, and G. Saito, J. Phys. Soc. Jpn. **65**, 1340 (1996).

[10] H. Morita, S. Watanabe, and M. Imada, J. Phys. Soc. Jpn. **71**, 2109 (2002).

[11] T. Koretsune, Y. Motome, and A. Furusaki, J. Phys. Soc. Jpn. **76**, 074719 (2007).

[12] T. Yoshioka, A. Koga, and N. Kawakami, Phys. Rev. Lett. **103**, 036401 (2009).

[13] B. Kyung and A.-M. S. Tremblay, Phys. Rev. Lett. **97**, 046402 (2006).

[14] R. T. Clay, H. Li, and S. Mazumdar, Phys. Rev. Lett. **101**, 166403 (2008).

[15] M. Abdel-Jawad, I. Terasaki, T. Sasaki, N. Yoneyama, N. Kobayashi, Y. Uesu, and C. Hotta, Phys. Rev. B **82**, 125119 (2010).

[16] H. Gomi, T. Imai, A. Takahashi, and M. Aihara, Phys. Rev. B **82**, 035101 (2010).

[17] K. Itoh, H. Itoh, M. Naka, S. Saito, I. Hosako, N. Yoneyama, S. Ishihara, T. Sasaki, and S. Iwai, Phys. Rev. Lett. **110**, 106401 (2013).

[18] M. Naka and S. Ishihara, J. Phys. Soc. Jpn. **82**, 023701 (2013).

[19] T.-K. Ng and P. A. Lee, Phys. Rev. Lett. **99**, 156402 (2007).

[20] S. Elsässer, D. Wu, M. Dressel, and J. A. Schlueter, Phys. Rev. B **86**, 155150 (2012).

[21] Y. Nakamura, N. Yoneyama, T. Sasaki, T. Tohyama, A. Nakamura, and H. Kishida, J. Phys. Soc. Jpn. **83**, 074708 (2014).

[22] Y. Shimizu, K. Miyagawa, K. Kanoda, M. Maesato, and G. Saito, Phys. Rev. B **73**, 140407(R) (2006).

[23] A. Kawamoto, Y. Honma, K. I. Kumagai, N. Matsunaga, and K. Nomura, Phys. Rev. B **74**, 212508 (2006).

[24] S. Nakajima, T. Suzuki, Y. Ishi, K. Ohishi, I. Watanabe, T. Goto, A. Oosawa, N. Yoneyama, N. Kobayashi, F. Pratt, and T. Sasaki, J. Phys. Soc. Jpn. **81**, 093706 (2012).

[25] M. de Souza, A. Brühl, Ch. Strack, B. Wolf, D. Schweitzer, and M. Lang, Phys. Rev. Lett. **99**, 037003 (2007).

[26] R. S. Manna, M. de Souza, A. Brühl, J. A. Schlueter, and M. Lang, Phys. Rev. Lett. **104**, 016403 (2010).

[27] M. Poirier, M. de Lafontaine, K. Miyagawa, K. Kanoda, and Y. Shimizu, Phys. Rev. B **89**, 045138 (2014).

[28] M. Naka and S. Ishihara, J. Phys. Soc. Jpn. **79**, 063707 (2010).

[29] C. Hotta, Phys. Rev. B **82**, 241104 (2010).

[30] K. Sedlmeier, S. Elsässer, D. Neubauer, R. Beyer, D. Wu, T. Ivek, S. Tomić, J. A. Schlueter, and M. Dressel, Phys. Rev. B **86**, 245103 (2012).

[31] M. Pinterić, M. Čulo, O. Milat, M. Basletić, B. Korin-Hamzić, E. Tafra, A. Hamzić, T. Ivek, T. Peterseim, K. Miyagawa, K. Kanoda, J. A. Schlueter, M. Dressel, and S. Tomić, Phys. Rev. B **90**, 195139 (2014).

[32] S. Tomić, M. Pinterić, T. Ivek, K. Sedlmeier, R. Beyer, D. Wu, J. A. Schlueter, D. Schweitzer, and M. Dressel, J. Phys.: Condens. Matter **25**, 436004 (2013).

[33] M. Pinterić, T. Ivek, M. Čulo, O. Milat, M. Basletić, B. Korin-Hamzić, E. Tafra, A. Hamzić, M. Dressel, and S. Tomić, Physica B: Condens. Matter **460**, 202 (2015).

[34] K. G. Padmalekha, M. Blankenhorn, T. Ivek, L. Bogani, J. A. Schlueter, and M. Dressel, Physica B: Condens. Matter **460**, 211 (2015).

[35] J. van den Brink and D. I. Khomskii, J. Phys.: Condens. Matter **20**, 434217 (2008).

[36] S. Ishihara, J. Phys. Soc. Jpn. **79**, 011010 (2010).

[37] S. Ishihara, J. Phys.: Condens. Matter **26**, 493201 (2014).

[38] T. Kimura, T. Goto, H. Shintani, K. Ishizaka, T. Arima, and Y. Tokura, Nature (London) **426**, 55 (2003).

[39] J. Wang, J. B. Neaton, H. Zheng, V. Nagarajan, S. B. Ogale, B. Liu, D. Viehland, V. Vaithyanathan, D. G. Schlom, U. V. Waghmare, N. A. Spaldin, K. M. Rabe, M. Wuttig, and R. Ramesh, Science **299**, 1719 (2003).

[40] P. Lunkenheimer, J. Müller, S. Krohns, F. Schrettle, A. Loidl, B. Hartmann, R. Rommel, M. de Souza, C. Hotta, J. A. Schlueter, and M. Lang, Nat. Mater. **11**, 755 (2012).

[41] N. Ikeda, H. Ohsumi, K. Ohwada, K. Ishii, T. Inami, K. Kakurai, Y. Murakami, K. Yoshii, S. Mori, Y. Horibe, and H. Kito, Nature (London) **436**, 1136 (2005).

[42] A. Nagano, M. Naka, J. Nasu, and S. Ishihara, Phys. Rev. Lett. **99**, 217202 (2007).

[43] M. Naka, A. Nagano, and S. Ishihara, Phys. Rev. B **77**, 224441 (2008).

[44] P. Monceau, F. Ya. Nad, and S. Brazovskii, Phys. Rev. Lett. **86**, 4080 (2001).

[45] H. Yoshioka, M. Tsuchiizu, and H. Seo, J. Phys. Soc. Jpn. **76**, 103701 (2007).

[46] Y. Otsuka, H. Seo, Y. Motome, and T. Kato, J. Phys. Soc. Jpn. **77**, 113705 (2008).

[47] K. Yamamoto, S. Iwai, S. Boyko, A. Kashiwazaki, F. Hiramatsu, C. Okabe, N. Nishi, and K. Yakushi, J. Phys. Soc. Jpn. **77**, 074709 (2008).

[48] P. Lunkenheimer, B. Hartmann, M. Lang, J. Müller, D. Schweitzer, S. Krohns, and A. Loidl, Phys. Rev. B **91**, 245132 (2015).

[49] H. Gomi, M. Ikenaga, Y. Hiragi, D. Segawa, A. Takahashi, T. J. Inagaki, and M. Aihara, Phys. Rev. B **87**, 195126 (2013).

[50] S. Dayal, R. T. Clay, H. Li, and S. Mazumdar, Phys. Rev. B **83**, 245106 (2011).

[51] T. Mori, H. Mori, and S. Tanaka, Bull. Chem. Soc. Jpn. **72**, 179 (1999).

[52] Y. Kawakami, S. Iwai, T. Fukatsu, M. Miura, N. Yoneyama, T. Sasaki, and N. Kobayashi, Phys. Rev. Lett. **103**, 066403 (2009).

[53] K. Yonemitsu, S. Miyashita, and N. Maeshima, J. Phys. Soc. Jpn. **80**, 084710 (2011).

[54] H. Gomi, T. Kawatani, T. J. Inagaki, and A. Takahashi, J. Phys. Soc. Jpn. **83**, 094714 (2014).

[55] B. J. Powell and R. H. McKenzie, Rep. Prog. Phys. **74**, 056501 (2011).

[56] E. Scriven and B. J. Powell, J. Chem. Phys. **130**, 104508 (2009).

[57] E. Scriven and B. J. Powell, Phys. Rev. B **80**, 205107 (2009).
[58] S. Miyashita and K. Yonemitsu, Phys. Rev. B **75**, 245112 (2007).
[59] Y. Tanaka and K. Yonemitsu, J. Phys. Soc. Jpn. **77**, 094712 (2008).
[60] M. Naka, J. Nasu, T. Watanabe, and S. Ishihara (unpublished).
[61] R. T. Clay, S. Mazumdar, and D. K. Campbell, Phys. Rev. B **67**, 115121 (2003).
[62] M. Kuwabara, H. Seo, and M. Ogata, J. Phys. Soc. Jpn. **72**, 225 (2003).
[63] T. Tatsumi, H. Gomi, A. Takahashi, Y. Hirao, and M. Aihara, J. Phys. Soc. Jpn. **81**, 034712 (2012).
[64] S. Iguchi, S. Sasaki, N. Yoneyama, H. Taniguchi, T. Nishizaki, and T. Sasaki, Phys. Rev. B **87**, 075107 (2013).